J Nanostruct 6(3): 184-189, Summer 2016

RESEARCH PAPER

Photodegradation of Acid Black 1 and Removing Heavy Metals from the Water by an Inorganic Nanocomposite Synthesized via Simple Co-Precipitation Method

Marziyeh Mohammadi, Mohammad Sabet, Fatemeh Googhari*

Department of Chemistry, Faculty of Science, Vali-e-Asr University of Rafsanjan, Rafsanjan, Iran

ARTICLE INFO

Article History:
Received 18 April 2016
Accepted 05 June 2016
Published 1 July 2016

Keywords:
Co-precipitation
Nanocomposite
Optical properties
Photocatalyst
Water treatment

ABSTRACT

In this experimental work, PbS/ZnS/ZnO nanocomposite was synthesized via a simple co-precipitation method. The effect of Zn^{2+}/Pb^{2+} mole ratio was investigated on the product size and morphology. The products were characterized via scanning electron microscopy to obtain product size and morphology. The optical properties of the nanocomposites were studied by ultra violet-visible spectroscopy. Photocatalytic activity of the product was examine by decomposition of acid black 1 as dye. To investigation of the effect of as synthesized nanocomposite on the water treatment, the influences of the nanocomposite to remove heavy ions was studied by atomic absorption spectroscopy. The results showed that the synthesized nanocomposite has well optical properties, photocatalytic and water treatment activities.

How to cite this article
Mohammadi M, Sabet M. Googhari Photodegradation of Acid Black 1 and Removing Heavy Metals from the Water by an Inorganic Nanocomposite Synthesized via Simple Co-Precipitation Method. J Nanostruct, 2016; 6(3):184-189. DOI: 10.7508/JNS.2016.03.002

INTRODUCTION

One of the important binary IV–VI semiconductor material is Lead sulfide (PbS) which have novel semiconducting and optical properties [1]. Even for relatively large structures, PbS shows strong quantum confinement due to its large exciton bohr radious [2, 3]. Until now different morphologies of lead sulfide are synthesized such as flower-like crystals [4], star shapes [5], dendrites [6], nanocubes [7], nanocrystals [8] and nanorods [9]. Another interesting semiconductor is ZnO that has great potentiality for being used in preparing solar cell [10, 11], varistors [12], gas sensors [13], electronic materials [14], chemical absorbent [15], electrostatic dissipative coating [16], catalysts for liquid phase hydrogenation [17], and catalysts for photo-catalytic degradation [18] instead of titania nanoparticles [19]. Until now, Different production methods such as chemical vapor deposition (CVD) [20] vapor phase oxidation [21], thermal vapor transport and condensation (TVTC) [22, 23], precipitation [24-26], sol–gel [27, 28], sonochemical methods [29], hydrothermal [30] and solvothermal [31][28] were served. ZnS is a member of wide band gap II–VI group semiconductors that has attracted attention due to various size-dependent properties of optics, electricity, magnetism, etc. With the progress of nanoscience, this material gained much attention for its interesting potential applications in optoelectronic, luminescence and biodiagnostics [32-35]. Various methods have been served, such as the single-source molecular precursor[36], the solvothermal and hydrothermal routes [37, 38], the chemical vapor deposition (CVD) method [36] the liquid–crystal template [39] and the g-irradiation route [40] to synthesize ZnS nanocrystals. There are a few research articles that deal with the synthesis of a nanocomposite contained from various semiconductors to use in degradation of

* Corresponding Author Email: M.sabet@vru.ac.ir

dye molecules and organic pollution. Also, there are few works related to use nanocomposite contained from different nanomaterials to use in water treatment activity. But in this work, we served a new nanocomposite to degradation dye molecules and also a good candidate to use in water treatment for removing heavy metal ions from the water. The results showed the synthesized nanocomposite has unique behavior in photodegradation and also water treatment activity. The main reason for this significant behavior is related to unique semiconducting properties of the nanomaterials and also high surface to volume ratio of them.

EXPERIMENTAL

All the chemicals reagents used in the experiments such as $Pb(NO_3)_2$, $Zn(NO_3)_3.9H_2O$, thiourea and NaOH were of analytical grade and used as received without further purification. XRD patterns were recorded by a Rigaku D-max C III, X-ray diffractometer using Ni-filtered Cu Kα radiation. Scanning electron microscopy (SEM) images were obtained on Philips XL-30ESEM equipped with an energy dispersive X-ray spectroscopy. UV-Vis spectra were recorded using a UV–Vis spectrophotometer (PerkinElmer).

To synthesis of the nanocomposite, a certain amount of $Pb(NO_3)_2$ Was dissolved in the distilled water to obtain a colorless solution. After the zinc solution was obtained from dissolving different amounts of $Zn(NO_3)_3.9H_2O$ respect to $Pb(NO_3)_2$ in the water. The final solution was obtained from a mixture of two solutions and adding 0.02 g of thiourea to the Zn/Pb solution. Then 0.01 g CTAB was added to the final solution as a surfactant. pH of the prepared solution was increased with NaOH solution to and after that, a precipitate was obtained. The precipitate was washed with distilled water and absolute ethanol several times and dried at 80 °C for 5 hours. Table 1 shows sample preparation conditions.

RESULT AND DISCUSSION

XRD pattern of the product was shown in Fig. 1. It can be seen that the pattern is mainly composed of three kinds peaks related to three compounds presented in the nanocomposite namely PbS, ZnS and ZnO. It can also be seen that there are no any other materials in the composites and hence the product is high pure. The peaks placed at 26.5°, 30.5°, 43.5°, 51°, 54°, 63°, 69° and 71° is belong to (111), (200), (220), (311), (222), (400), (331), (420), (422) miller indices related to PbS compound with cubic phase (JCPDS= 002-1431). The peaks of ZnS compound with hexagonal phase placed at 27.5°, 30.5°, 51.5° and 63.3° that is related to (100), (101), (103) and (202) miller indices (JCPDS= 01-075-1547). Other peaks are related to ZnO compound with hexagonal phase (JCPDS=01-075-1533). There are also ZnO peaks overlapped with some ZnS compound.

The effect of Zn^{2+}:Pb^{2+} mole ratio on the nanocomposite size and morphology was investigated by SEM image. When the mole ratio

Table 1. The samples preparation conditions.

Sample No	Zn^{2+}:Pb^{2+} mole ratio
1	1:1
2	1:2
3	1:3
4	1:4
5	1:5

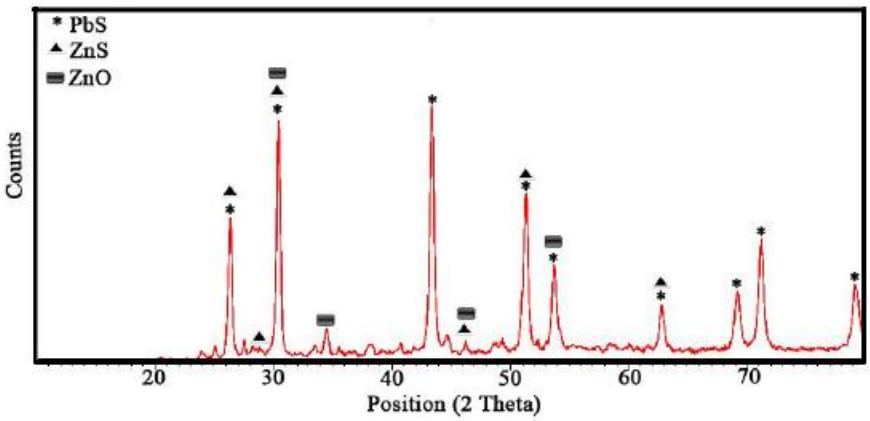

Fig. 1. XRD pattern of the nanocomposite

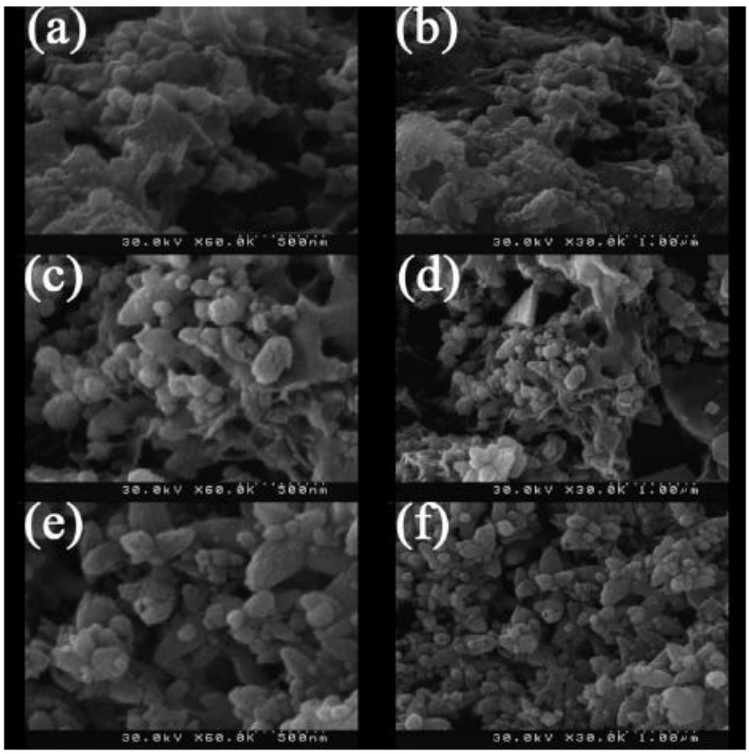

Fig. 2. SEM image of (a,b) sample No. 1, (c,d) sample No. 2 and (e, f) sample No. 3, respectively.

was selected to 1:1, the product was mainly composed of irregular and large shapes (Fig. 2a, b). Also, the product is composed of tiny particles aggregated together. It can be said that in this mole ratio, a number of cations for reacting with S^{2-} is low and hence the cations (Pb^{2+} and Zn^{2+}) have enough time to react with S^{2-} and therefore, large shapes are created.

When the mole ratio was increased to 1:2, the particle size was decreased that is mainly due to an increase of cations amount (Fig. 2c, d). In fact, when the amount of Pb^{2+} is increased in the reaction medium, the nucleation centers is enhanced and hence more nucleus with smaller size are obtained. There is also some large particles that is due to aggregation of tiny particles. In other words, due to the high surface energy of the nanoparticles, they aggregated together and hence larger particles were achieved.

Fig. 2e, f shows SEM image of PbS/ZnS/ZnO nanocomposite prepared with Zn^{2+}/Pb^{2+} 1:3 mole ratio. As shown in this figure, flower-like nanostructures were achieved. In fact, when the mole ratio was increased to 1:3, the amount of Pb^{2+} for reaction with S^{2-} was increased. Therefore, the number of nucleuses was increased to the synthesis of all of PbS, ZnS and ZnO particles and hence tiny particles were achieved. After that due to the diffusion process, flower-like structures were obtained.

The increase of the mole ratio to 1:4 lead to the creation of the nanocomposite with very tiny particles that is mainly due to an increase of nucleation centers (Fig. 3a, b). There are also very large irregular shapes that are due to aggregation of nanoparticles. By increasing the mole ratio to 1:5, the particle size was decreased that is due to higher nucleation centers in the reaction medium (Fig. 3c, d).

Fig. 4 shows UV-Vis spectra of the as-synthesized nanocomposites. It can be seen that each compound showed unique absorption behavior. As shown in this figure, by increasing the PbS-ZnS mole ratio, the absorption edge moves to a higher wavelength. In fact, by increase the amount of lead source, the produce of lead sulfide is increased and hence due to the lower band gap of PbS respect to the ZnS and ZnO, the nanocomposite can absorb more light radiation. In other words by increasing the amount of Pb^{2+} source, the amount of PbS is increased and due to a linear combination of the orbital molecular

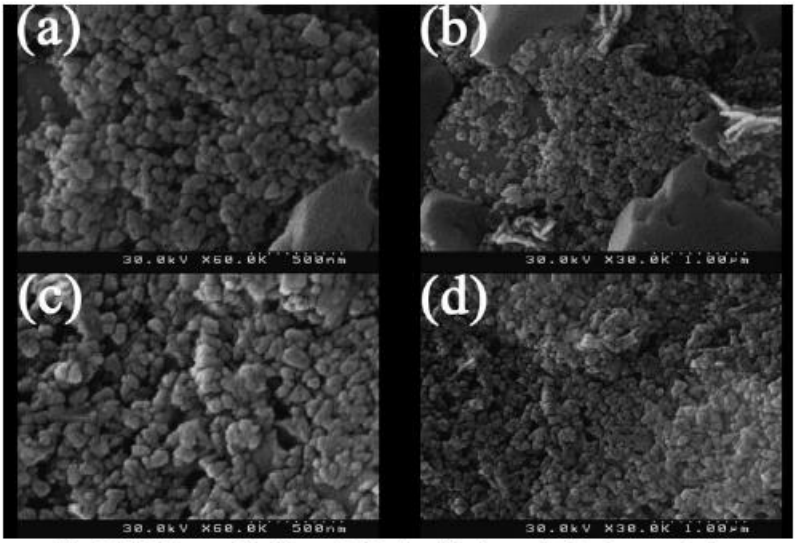

Fig. 3. SEM image of (a, b) sample No. 4 and (c,d) sample No. 5, respectively.

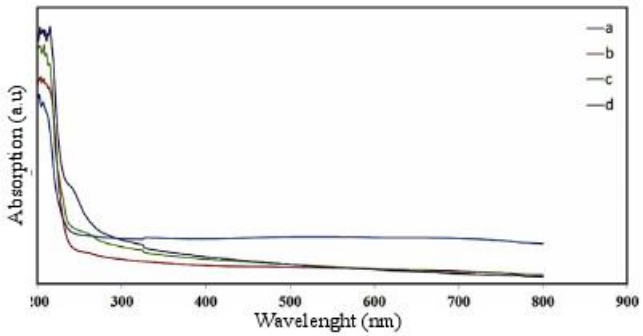

Fig. 4 (a-d). UV-Vis spectra of the sample No. 1-4, respectively.

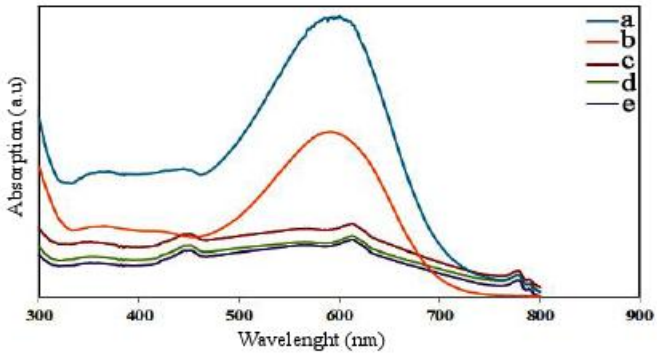

Fig. 5. UV-Vis of Acid Black 1 (a), dye solution contain nanocomposite at 0 min (b), 20 min (c), 40 min (d) and 60 min (e) radiation.

of each compound, they can adsorb more light radiation.

To investigate the photocatalytic effect of the synthesized nanocomposite, destruction of acid black was studied under ultra-violet radiation (Fig. 5). It can be seen that the product can destruct the dye in large quantities. This is mainly due to the synergetic effect of each compound respect to the other one to decompose of the acid black structure. In fact, when the light exposed to the dye solution contained the nanocomposite, the number of electron-hole pairs was rather

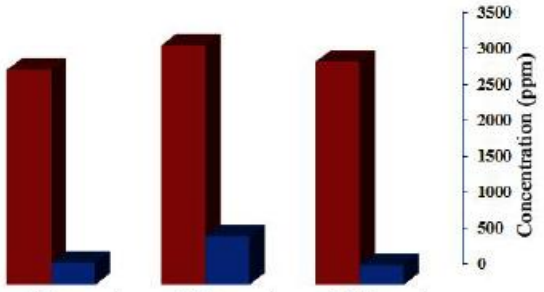

	Zn^{2+}	Pb^{2+}	Cd^{2+}
After treatment	299.166	672.95	270.301
Before treatment	2974.8	3312	3084.7

Fig. 6. Water treatment performance of the nanocomposite.

than each compound singly and therefore dye molecules were destructive in large amount. It can be also seen that the dye molecules was decomposed in the first moment before they exposed to the UV light radiation. It can be concluded that the nanocomposite has excellent photocatalytic activity only in the visible range of the exposed light.

To investigate of water treatment behavior of the as-synthesized nanocomposite, the activity of the nanocomposite to remove heavy metal ions from the water was studied (Fig. 6). For this purpose, three solutions contain Cd^{2+}, Pb^{2+} and Zn^{2+} ions with 0.01 molar concentration were prepared and then a certain amount of nanocomposite was poured into each solution separately under vigorous stirring. After one hour, the solutions were centrifuged and studied by atomic absorption spectroscopy to find remain ions in the water. The results showed that the nanocomposite has significant adsorption value, and it could remove about percent of heavy ions from the water. The table shows the ions concentration before and after pouring the nanocomposite. In fact due to high surface to volume ratio of the nanoparticles, their surface can adsorb heavy ions in the aqueous medium.

CONCLUSION

In this experimental work, we synthesized PbS/ZnS/ZnO nanocomposite via a simple co-precipitation method. The effect of Zn^{2+}:Pb^{2+} mole ratio was investigated on the product size and morphology and it was found that by increasing the amount of zinc source respect to the lead one, the particles size is decreased. The optical properties of the as-synthesized nanocomposite were studied by UV-Vis spectra. It was found by increasing the Zn^{2+}:Pb^{2+} mole ratio, the absorption shift to the higher wavelength that is mainly due to decrease the particles size. The photocatalytic activity of the nanocomposite was investigated by decomposition of acid black 1 as a dye. The results showed that the nanocomposite destructive dye structure in high quantities. The main reason is a linear combination of the compounds molecular orbitals with each other. The activity of the product to remove heavy ions from the water medium was investigated by atomic adsorption spectroscopy. The results showed that the nanocomposite can adsorb heavy metal ions from the water through surface adsorption. In fact, due to high surface atoms of nanomaterials respect to the bulk one, they are more active than the bulk materials and hence they can adsorb more heavy ions from the water medium.

CONFLICT OF INTEREST

The authors declare that there is no conflict of interests regarding the publication of this manuscript.

REFERENCES

1. Qin A-M, Fang Y-P, Zhao W-X, Liu H-Q, Su C-Y. Directionally dendritic growth of metal chalcogenide crystals via mild template-free solvothermal method. J Cryst Growth. 2005; 283(1): 230-241.
2. Zhou S, Feng Y, Zhang L. Sonochemical synthesis of large-scale single-crystal PbS nanorods. J Mater Res. 2003; 18(05): 1188-1191.
3. Dutta AK, Ho T, Zhang L, Stroeve P. Nucleation and growth of lead sulfide nano-and microcrystallites in supramolecular polymer assemblies. Chem Mater. 2000; 12(4): 1042-1048.
4. Ni Y, Wang F, Liu H, Yin G, Hong J, Ma X, et al. A novel aqueous-phase route to prepare flower-shaped PbS micron crystals. J Cryst Growth. 2004; 262(1): 399-402.
5. Zhou G, Lü M, Xiu Z, Wang S, Zhang H, Zhou Y, et al. Controlled synthesis of high-quality PbS star-shaped dendrites, multipods, truncated nanocubes, and nanocubes and their

shape evolution process. The Journal of Physical Chemistry B. 2006; 110(13): 6543-6548.
6. Zhang Z, Lee SH, Vittal JJ, Chin WS. A simple way to prepare PbS nanocrystals with morphology tuning at room temperature. The Journal of Physical Chemistry B. 2006; 110(13): 6649-6654.
7. Zhang W, Yang Q, Xu L, Yu W, Qian Y. Growth of PbS crystals from nanocubes to eight-horn-shaped dendrites through a complex synthetic route. Mater Lett. 2005; 59(27): 3383-3388.
8. Gautam UK, Seshadri R. Preparation of PbS and PbSe nanocrystals by a new solvothermal route. Mater Res Bull. 2004; 39(4): 669-676.
9. Saraidarov T, Reisfeld R, Sashchiuk A, Lifshitz E. Synthesis and characterization of PbS nanorods and nanowires. Physica E: Low-dimensional Systems and Nanostructures. 2007; 37(1): 173-177.
10. Wang Z-S, Huang C-H, Huang Y-Y, Hou Y-J, Xie P-H, Zhang B-W, et al. A highly efficient solar cell made from a dye-modified ZnO-covered TiO2 nanoporous electrode. Chem Mater. 2001; 13(2): 678-682.
11. Westermark K, Rensmo H, Lees AC, Vos JG, Siegbahn H. Electron spectroscopic studies of bis-(2, 2'-bipyridine)-(4, 4'-dicarboxy-2, 2'-bipyridine)-ruthenium (II) and bis-(2, 2'-bipyridine)-(4, 4'-dicarboxy-2, 2'-bipyridine)-osmium (II) adsorbed on nanostructured TiO2 and ZnO surfaces. The Journal of Physical Chemistry B. 2002; 106(39): 10108-10113.
12. Singhai M, Chhabra V, Kang P, Shah D. Synthesis of ZnO nanoparticles for varistor application using Zn-substituted aerosol OT microemulsion. Mater Res Bull. 1997; 32(2): 239-247.
13. Lin H-M, Tzeng S-J, Hsiau P-J, Tsai W-L. Electrode effects on gas sensing properties of nanocrystalline zinc oxide. Nanostruct Mater. 1998; 10(3): 465-477.
14. Feldmann C. Polyol-Mediated Synthesis of Nanoscale Functional Materials. Adv Funct Mater. 2003; 13(2): 101-107.
15. Rosso I, Galletti C, Bizzi M, Saracco G, Specchia V. Zinc oxide sorbents for the removal of hydrogen sulfide from syngas. Industrial & Engineering Chemistry Research. 2003; 42(8): 1688-1697.
16. Kitano M, Shiojiri M. Benard convection ZnO/resin lacquer coating—a new approach to electrostatic dissipative coating. Powder Technol. 1997; 93(3): 267-273.
17. Hamminga GM, Mul G, Moulijn JA. Real-time in situ ATR-FTIR analysis of the liquid phase hydrogenation of γ-butyrolactone over Cu-ZnO catalysts: A mechanistic study by varying lactone ring size. Chem Eng Sci. 2004; 59(22): 5479-5485.
18. Curri M, Comparelli R, Cozzoli P, Mascolo G, Agostiano A. Colloidal oxide nanoparticles for the photocatalytic degradation of organic dye. Materials Science and Engineering: C. 2003; 23(1): 285-289.
19. Fotou GP, Pratsinis SE. Photocatalytic destruction of phenol and salicylic acid with aerosol-made and commercial titania powders. Chem Eng Commun. 1996; 151(1): 251-269.
20. Wu J-J, Liu S-C. Catalyst-free growth and characterization of ZnO nanorods. The Journal of Physical Chemistry B. 2002; 106(37): 9546-9551.
21. Hu J, Li Q, Wong N, Lee C, Lee S. Synthesis of uniform hexagonal prismatic ZnO whiskers. Chem Mater. 2002; 14(3): 1216-1219.
22. Lao J, Huang J, Wang D, Ren Z. ZnO nanobridges and nanonails. Nano Lett. 2003; 3(2): 235-238.
23. Lao JY, Wen JG, Ren ZF. Hierarchical ZnO nanostructures. Nano Lett. 2002; 2(11): 1287-1291.
24. Pesika NS, Hu Z, Stebe KJ, Searson PC. Quenching of growth of ZnO nanoparticles by adsorption of octanethiol. The Journal of Physical Chemistry B. 2002; 106(28): 6985-6990.
25. Radovanovic PV, Norberg NS, McNally KE, Gamelin DR. Colloidal transition-metal-doped ZnO quantum dots. J Am Chem Soc. 2002; 124(51): 15192-15193.
26. Seelig EW, Tang B, Yamilov A, Cao H, Chang R. Self-assembled 3D photonic crystals from ZnO colloidal spheres. Mater Chem Phys. 2003; 80(1): 257-263.
27. Hoyer P, Weller H. Potential-dependent electron injection in nanoporous colloidal ZnO films. The Journal of Physical Chemistry. 1995; 99(38): 14096-14100.
28. Paul G, Bandyopadhyay S, Sen S, Sen S. Structural, optical and electrical studies on sol–gel deposited Zr doped ZnO films. Mater Chem Phys. 2003; 79(1): 71-75.
29. Qian D, Jiang J, Hansen PL. Preparation of ZnO nanocrystals via ultrasonic irradiation. Chem Commun. 2003; (9): 1078-1079.
30. Cheng B, Samulski ET. Hydrothermal synthesis of one-dimensional ZnO nanostructures with different aspect ratios. Chem Commun. 2004; (8): 986-987.
31. Jia Z, Yue L, Zheng Y, Xu Z. Rod-like zinc oxide constructed by nanoparticles: synthesis, characterization and optical properties. Mater Chem Phys. 2008; 107(1): 137-141.
32. Xia Y, Yang P, Sun Y, Wu Y, Mayers B, Gates B, et al. One-dimensional nanostructures: synthesis, characterization, and applications. Adv Mater. 2003; 15(5): 353-389.
33. Xiong Q, Chen G, Acord J, Liu X, Zengel J, Gutierrez H, et al. Optical properties of rectangular cross-sectional ZnS nanowires. Nano Lett. 2004; 4(9): 1663-1668.
34. Yao WT, Yu SH, Pan L, Li J, Wu QS, Zhang L, et al. Flexible Wurtzite-Type ZnS Nanobelts with Quantum-Size Effects: a Diethylenetriamine-Assisted Solvothermal Approach. small. 2005; 1(3): 320-325.
35. Salavati-Niasari M, Davar F, Seyghalkar H, Esmaeili E, Mir N. Novel inorganic precursor in the controlled synthesis of zinc blend ZnS nanoparticles via TGA-assisted hydrothermal method. CrystEngComm. 2011; 13(8): 2948-2954.
36. Liu J, Yan P, Yue G, Kong L, Zhuo R, Qu D. Synthesis of doped ZnS one-dimensional nanostructures via chemical vapor deposition. Mater Lett. 2006; 60(29): 3471-3476.
37. Wang H, Chen Z, Cheng Q, Yuan L. Solvothermal synthesis and optical properties of single-crystal ZnS nanorods. J Alloys Compd. 2009; 478(1): 872-875.
38. Wang L, Chen L, Luo T, Qian Y. A hydrothermal method to prepare the spherical ZnS and flower-like CdS microcrystallites. Mater Lett. 2006; 60(29): 3627-3630.
39. Zhu Y-C, Bando Y, Xue D-F. Spontaneous growth and luminescence of zinc sulfide nanobelts. Appl Phys Lett. 2003; 82: 1769.
40. Zhang D, Qi L, Cheng H, Ma J. Preparation of ZnS nanorods by a liquid crystal template. J Colloid Interface Sci. 2002; 246(2): 413-416.